Figures and figure supplements

Fracture healing is delayed in the absence of gasdermin-interleukin-1 signaling

Kai Sun *et al*
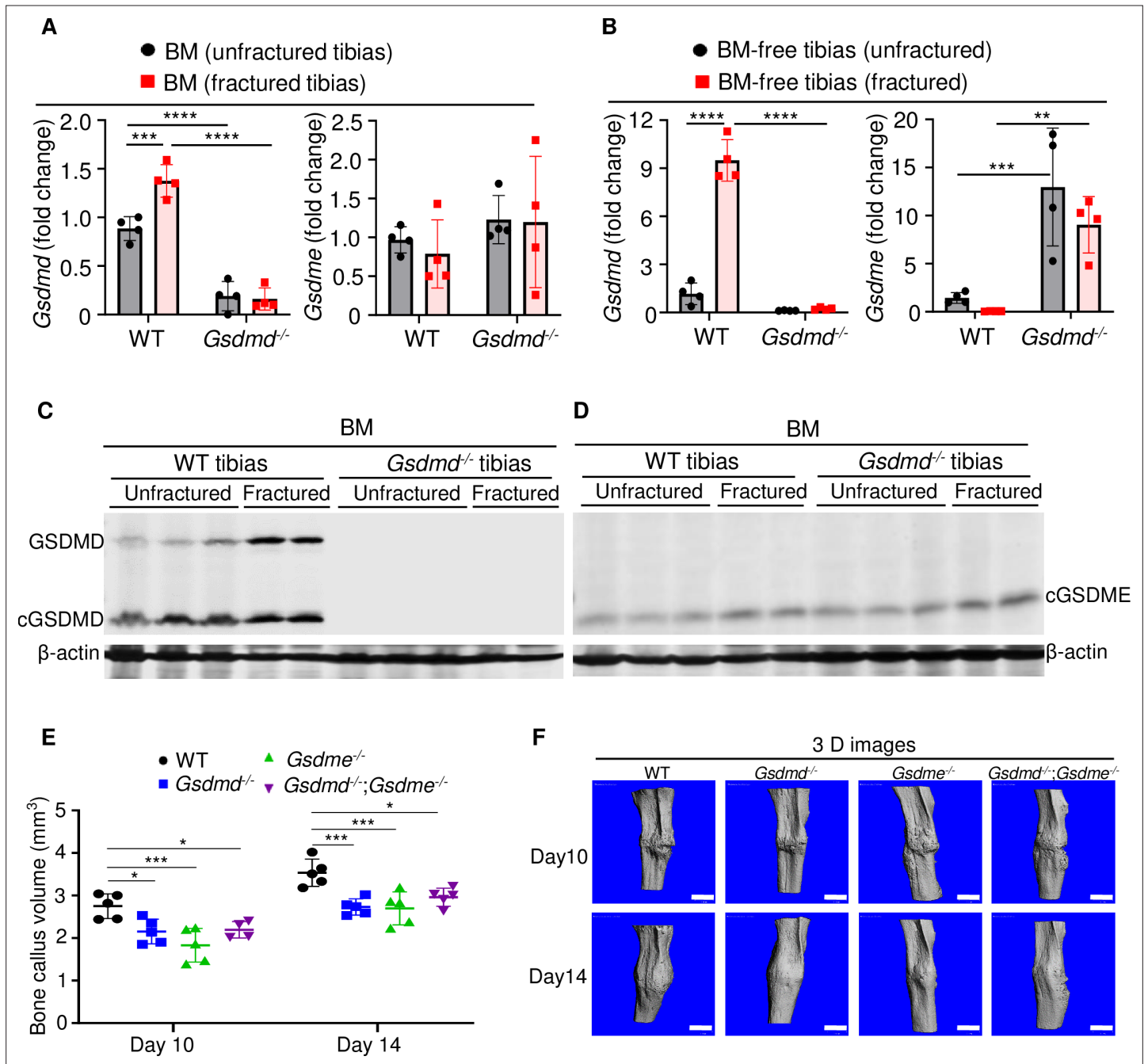
Figure 1. GSDMD and GSDME were expressed in bone microenvironment and involved in bone callus formation. (**A, C–D**) BM and (**B**) BM-free tibias from 12-week-old male WT and *Gsdmd*−/− mice (n = 4–5 mice). Samples were isolated from unfractured or fractured tibias (3 days after injury). (**A–B**) qPCR and (**C–D**) Western blot analyses. qPCR data were normalized to unfractured WT. (**E**) Bone callus volume was quantified using Scanco software (n = 5). (**F**) Representative 3D reconstructions of bones using μCT. Data were mean ± SD and are representative of at least three independent experiments. Data from male and female mice were pooled because there was no sex difference. **p < 0.01; ***p < 0.001; ****p < 0.0001, two-way ANOVA with Tukey's multiple comparisons test. Scale bar, 1 mm. BM, bone marrow; μCT, micro-computed tomography; WT, wild-type.
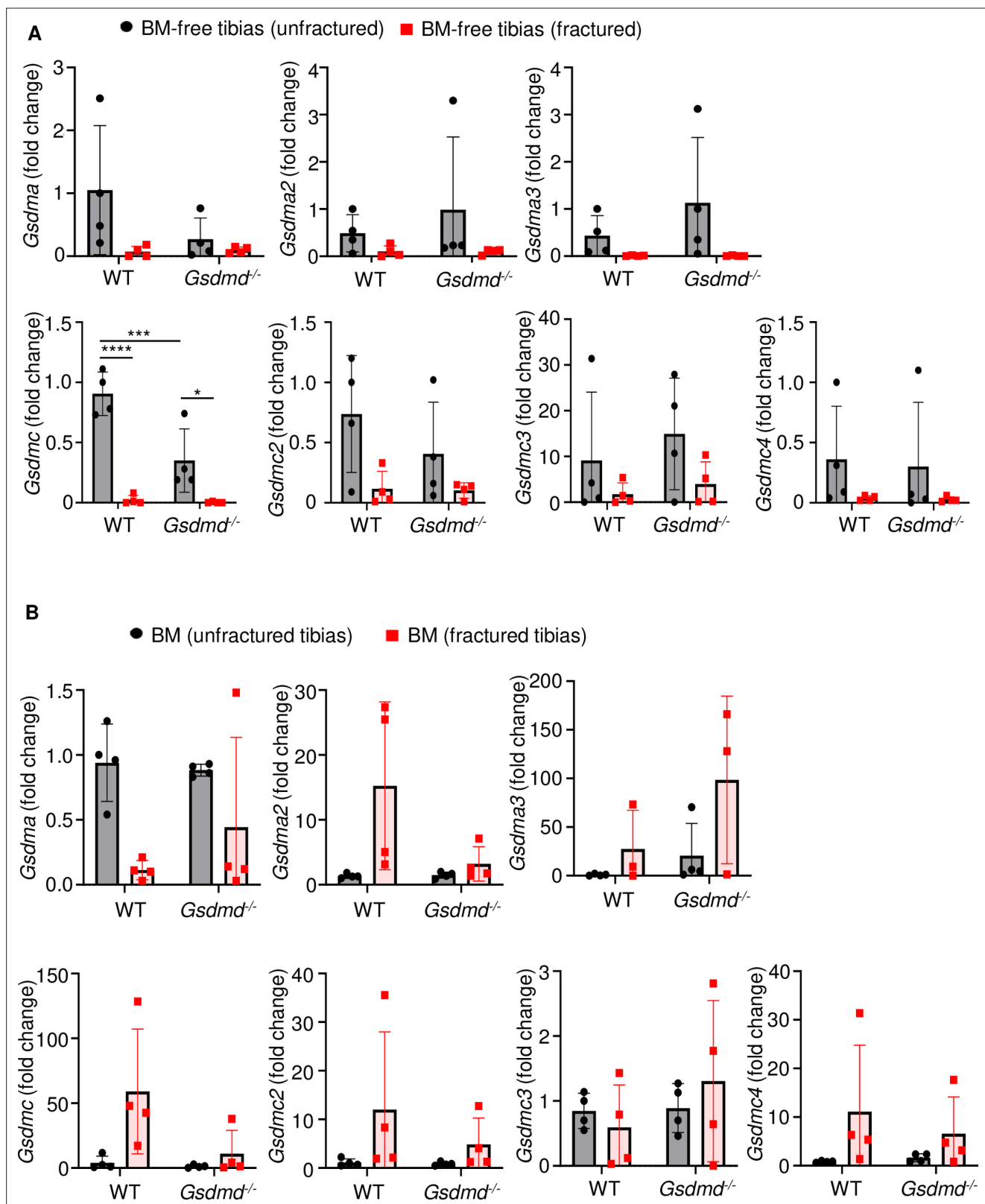
Figure 1—figure supplement 1. Several gasdermin (GSDM) family members were barely expressed in bones. RNAs were isolated from (**A**) bone marrow (BM)-free bones or (**B**) BM and were from 12-week-old male wild-type (WT) or *Gsdmd*−/− mice (n = 4–5). Samples were isolated from unfractured or fractured tibias (3 days after injury). qPCR (**A–B**) analysis. Data were normalized to unfractured WT, and were mean ± SD. *p < 0.05; ***p < 0.001; ****p < 0.0001, two-way ANOVA with Tukey's multiple comparisons test.
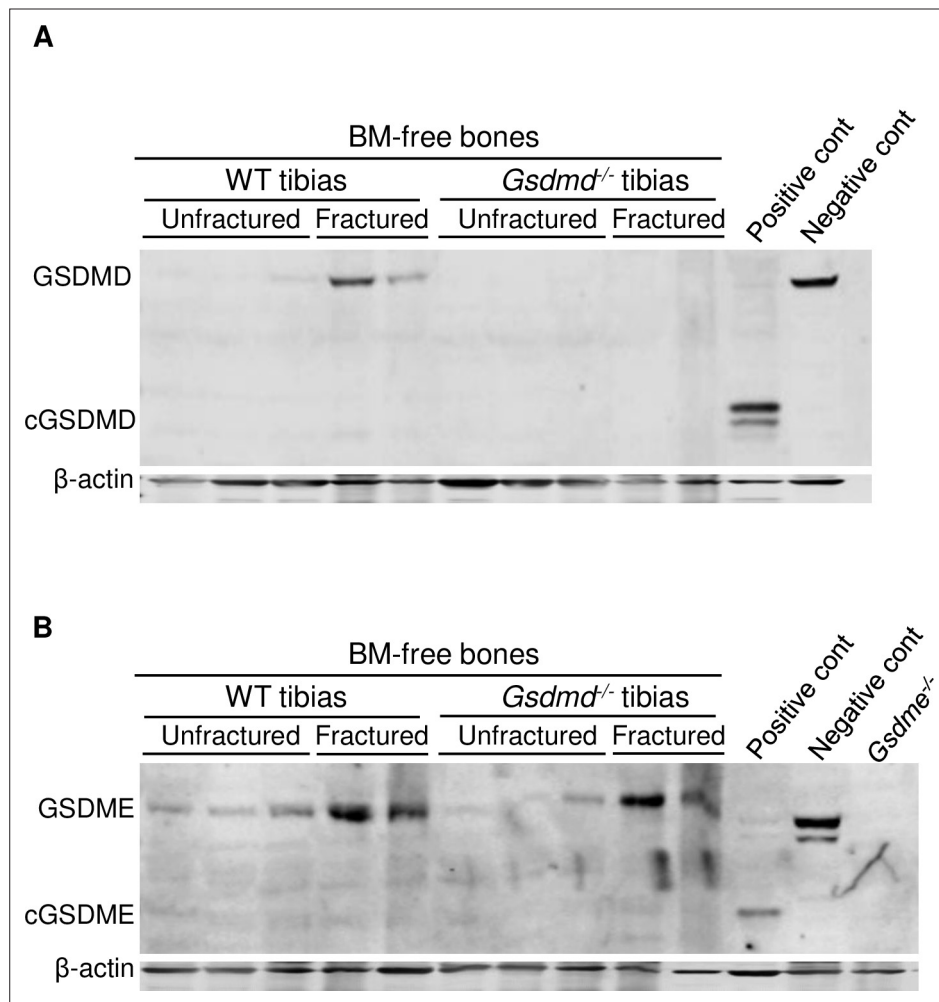
Figure 1—figure supplement 2. Fracture-induced GSDMD and GSDME expression. Proteins were isolated from bone marrow (BM)-free tibias from 12-week-old male wild-type (WT) or *Gsdmd−/−* mice. Tibias were unfractured or fractured (3 days after injury). GSDMD (**A**) and GSDME (**B**) were analyzed by immunoblotting. cGSDMD, cleaved GSDMD; cGSDME, cleaved GSDME; WT, wild-type.
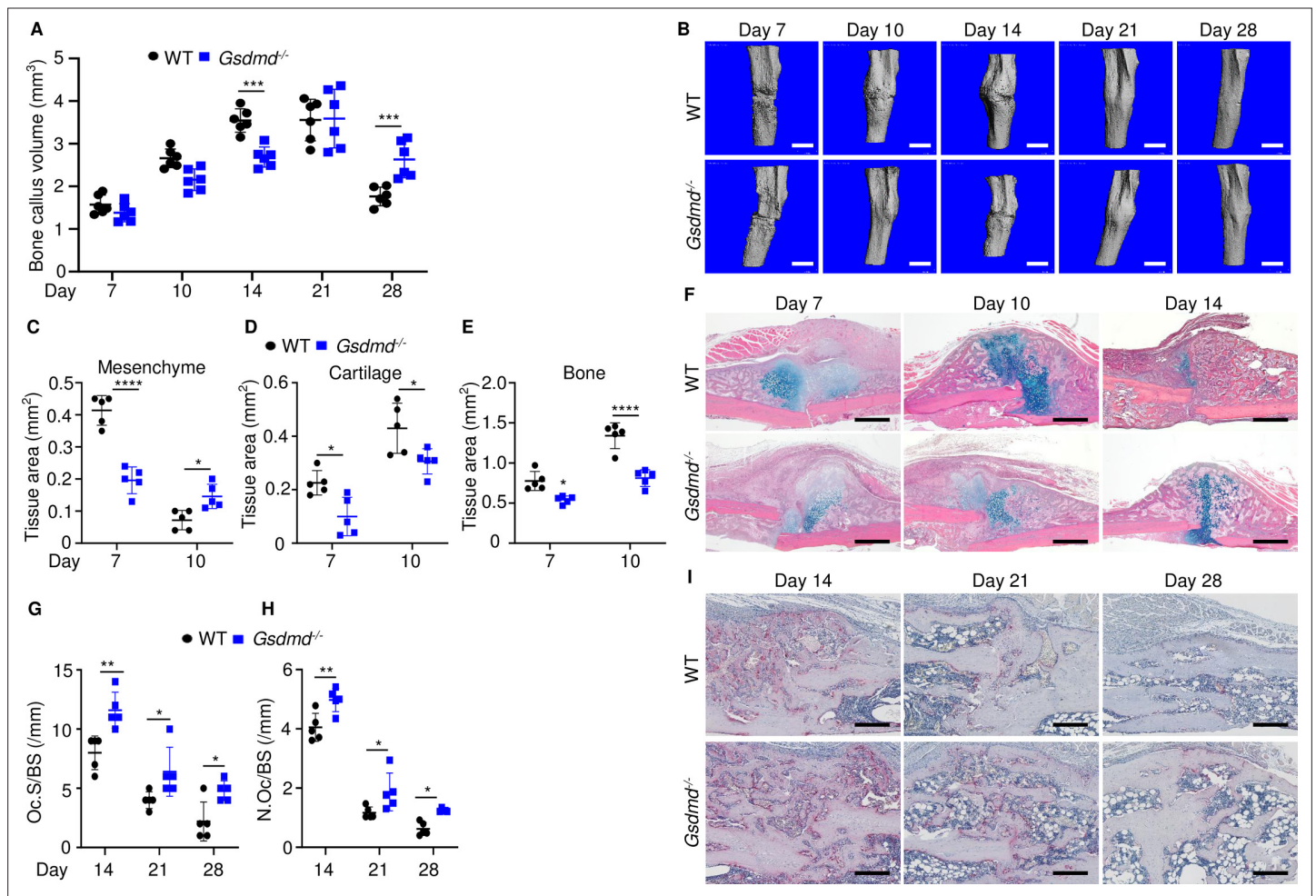
Figure 2. Loss of GSDMD delayed fracture healing. Tibias of 12-week-old male and female WT or *Gsdmd*⁻/⁻ mice were subjected to fracture and analyzed at the indicated times. (**A**) Bone callus volume was quantified using Scanco software (n = 6). (**B**) Representative 3D reconstructions of bones using µCT. (**C–E**) Quantification of tissue area by ImageJ software (n = 5). (**F**) Representative ABH staining. Quantification of Oc.S/BS (**G**) and N.Oc/BS (**H**) using Bioquant software (n = 5). (**I**) Representative images of TRAP staining. Data were mean ± SD. Data from male and female mice were pooled because there was no sex difference. *p < 0.05; ***p < 0.001; ****p < 0.0001, two-way ANOVA with Tukey's multiple comparisons test. Scale bar, 1 mm (**B**), 500 µm (**F**) ,or 200 µm (**I**). µCT, micro-computed tomography; WT, wild-type.
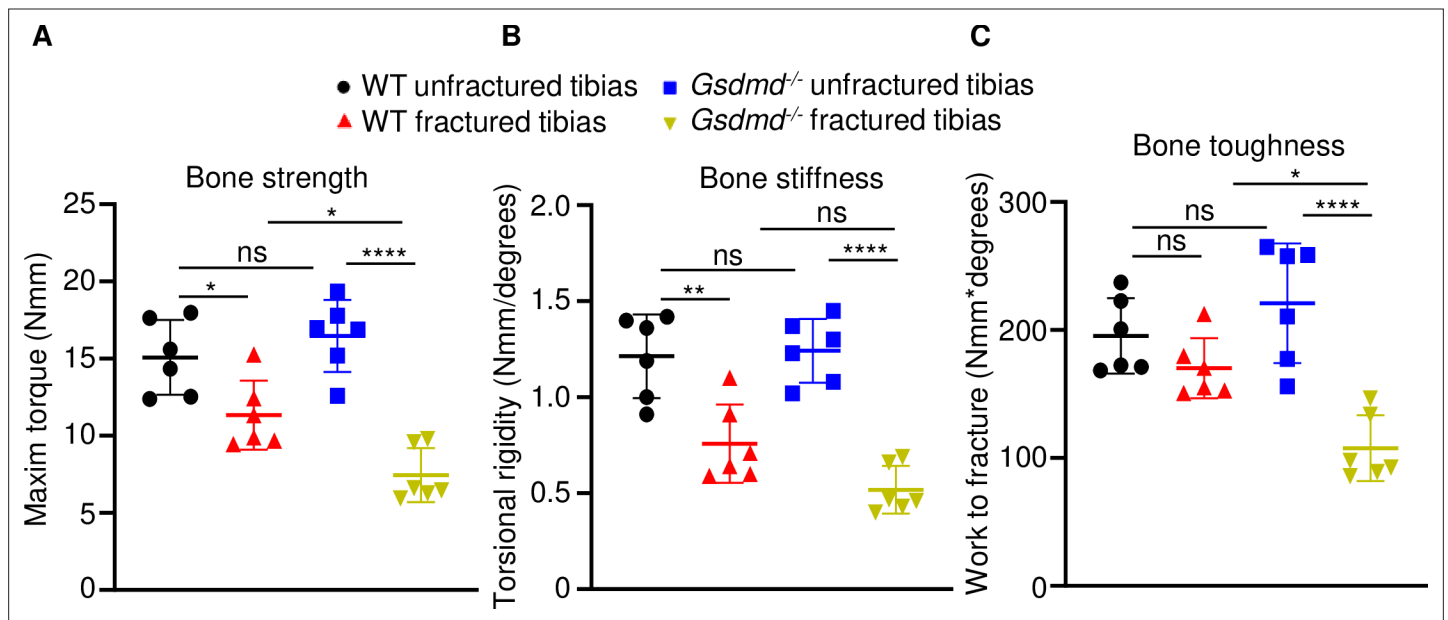
Figure 3. Loss of GSDMD compromised bone biomechanical properties after fracture. Unfractured or fractured tibias (28 days after injury) from 12-week-old male WT or *Gsdmd⁻/⁻* mice were subjected to a torsion test (n = 6). (**A**) Bone strength. (**B**) Bone stiffness. (**C**) Bone toughness. Data were mean ± SD. *p < 0.05; **p < 0.01; ****p < 0.0001; one-way ANOVA with Tukey's multiple comparisons test; ns, non significant; WT, wild-type.
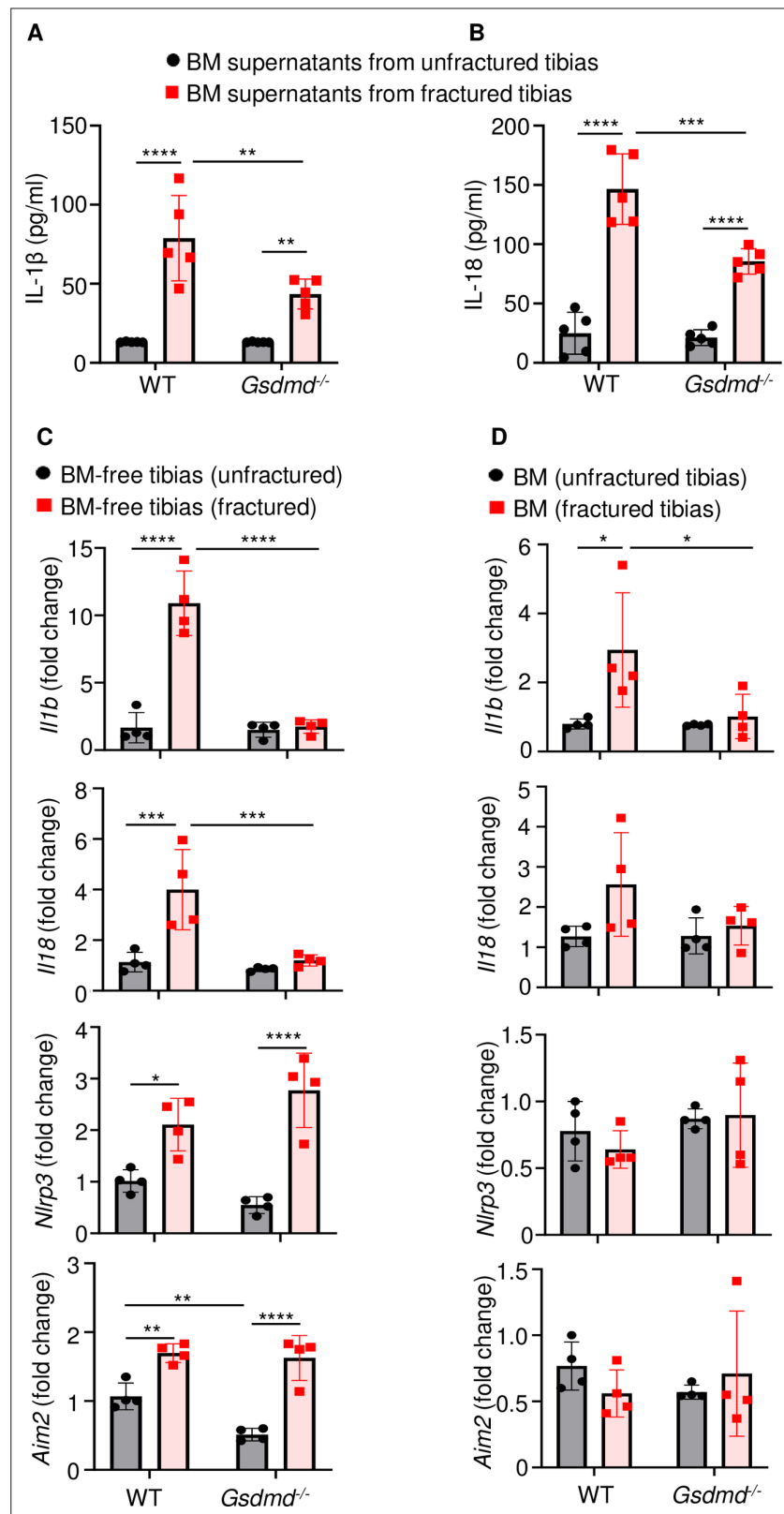
Figure 4. Loss of GSDMD attenuated the expression and secretion of interleukin-1β (IL-1β) and IL-18 induced by fracture. (**A–B**) BM supernatants and (**C**) BM-free bones were from 12-week-old male WT or *Gsdmd⁻/⁻* mice (n = 4–5). Samples were isolated from unfractured or fractured tibias (1 day after injury). (**A–B**) ELISA and (**C–D**) qPCR analyses. qPCR data were normalized to unfractured WT. Data were mean ± SD. *p < 0.05; **p < 0.01;

Figure 4 continued on next page

Figure 4 continued

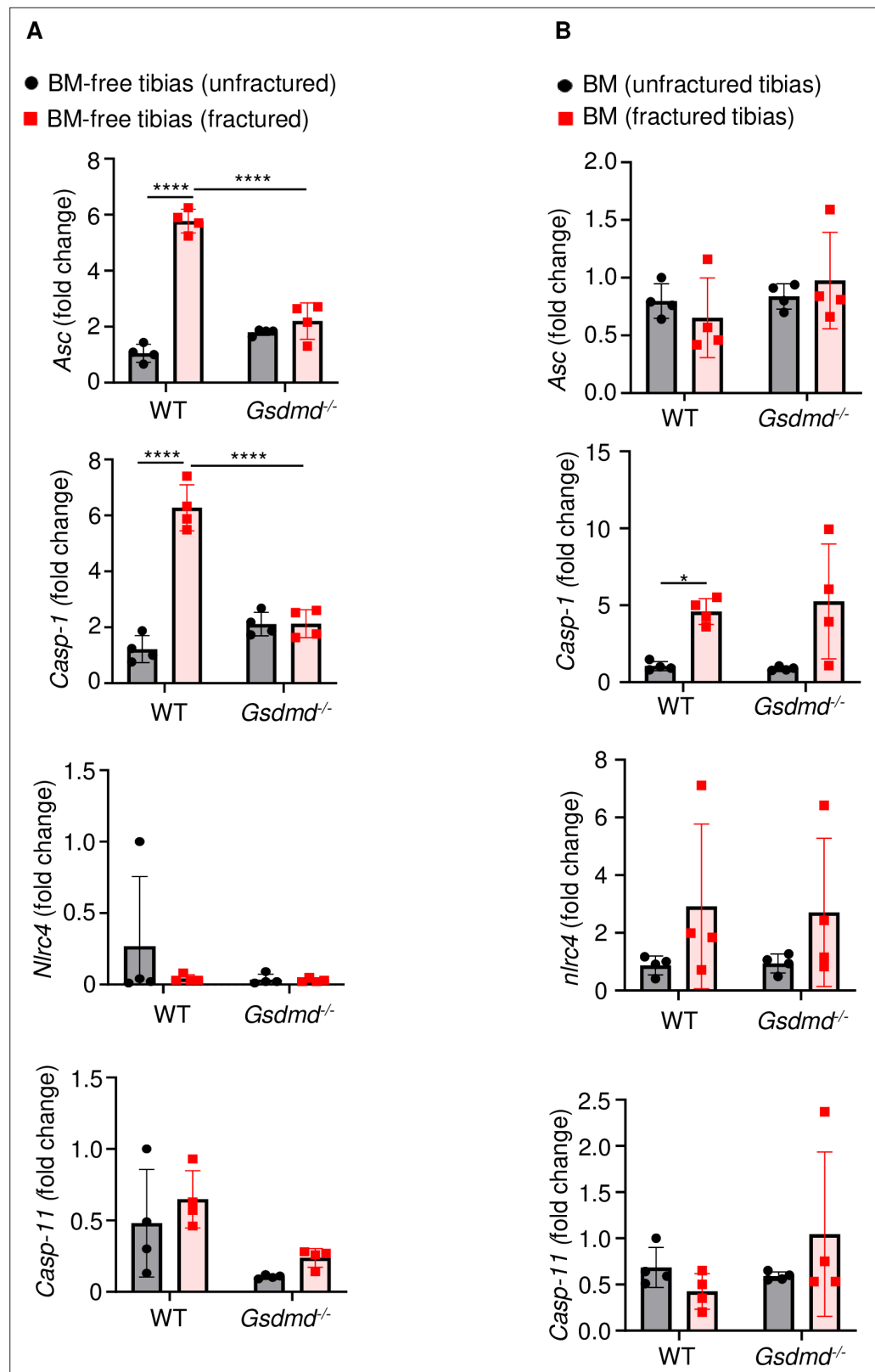***p < 0.001; ****p < 0.0001, two-way ANOVA with Tukey's multiple comparisons test. BM, bone marrow; WT, wild-type.

Figure 4—figure supplement 1. Fracture induced the expression of certain inflammasome components. RNAs were isolated from (**A**) BM-free bones or (**B**) BM were from 12-week-old male WT or *Gsdmd*^{-/-} mice (n = 4). Tibias were unfractured or fractured (3 days after injury). RNAs were analyzed by qPCR. Data were normalized to unfractured WT, and were mean ± SD. *p < 0.05; ***p < 0.001; ****p < 0.0001, two-way ANOVA with Tukey's multiple comparisons test. BM, bone marrow; WT, wild-type.
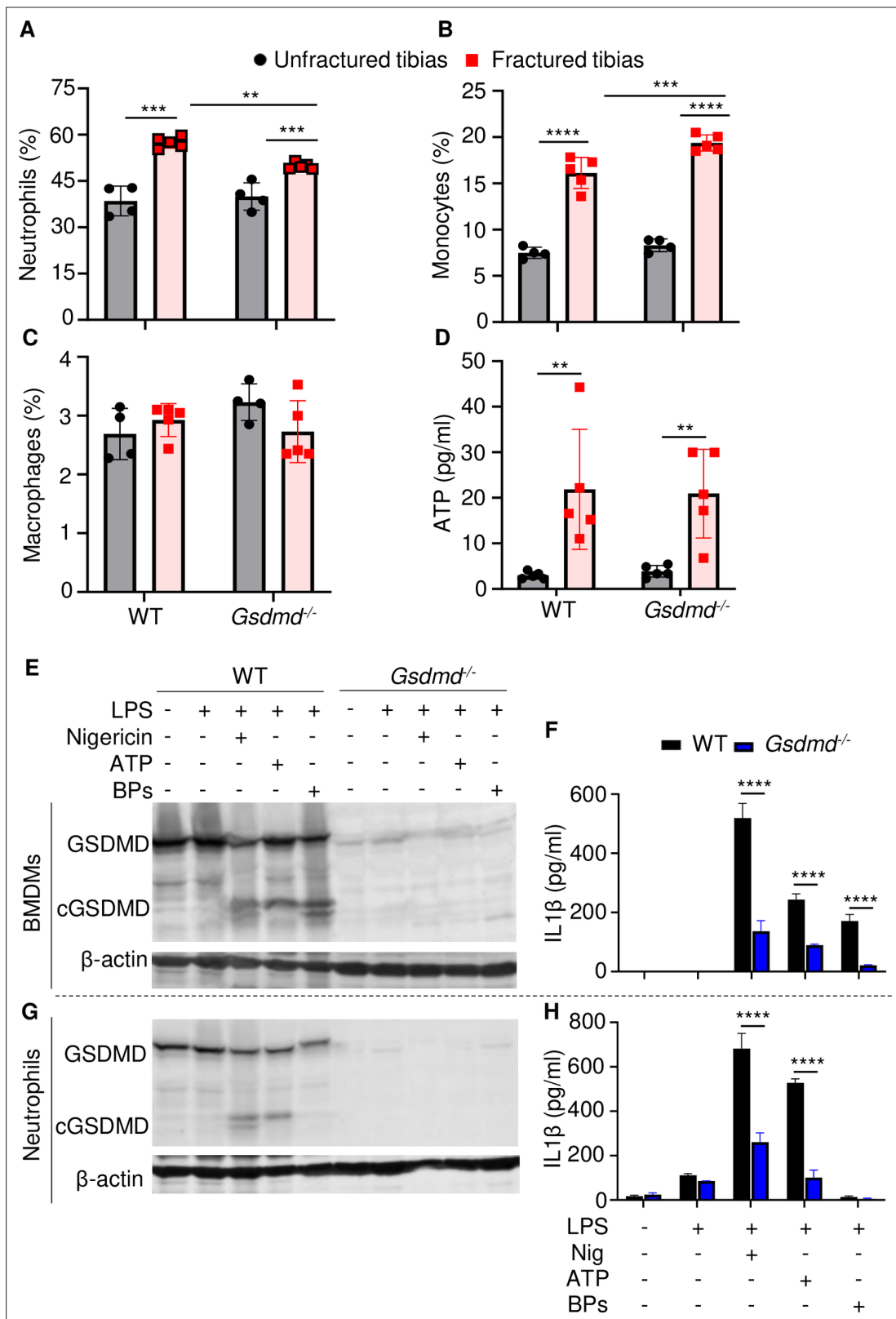
Figure 5. Loss of GSDMD attenuated the secretion of interleukin-1β (IL-1β) and IL-18 induced by danger signals. Cells were isolated from the tibias from 12-week-old female WT or *Gsdmd*−/− mice. (A–C) Cell counts (n = 4–5). BM was harvested from unfractured or fractured tibias (2 days after fracture). (D) ATP levels. BM supernatants were harvested from unfractured or fractured tibias (24 hr after fracture). (E–G) Immunoblotting analysis of GSDMD cleavage or (F–H) IL-1β ELISA run in triplicates. Bone marrow-derived macrophages (BMDMs) were expanded in vitro whereas neutrophils were

Figure 5 continued on next page

Figure 5 continued

immediately after purification. Cells were primed with 100 ng/ml LPS for 3 hr, then with 15 µM nigericin for 1 hr, 5 mM ATP for 1 hr, or 50 mg/ml bone particles for 2 hr. Data are mean ± SD and were representative of at least three independent experiments. *$p < 0.05$; **$p < 0.01$; ***$p < 0.001$; ****$p < 0.0001$, two-way ANOVA with Tukey's multiple comparisons test. BPs, bone particles; cGSDMD, cleaved GSDMD; WT, wild-type.
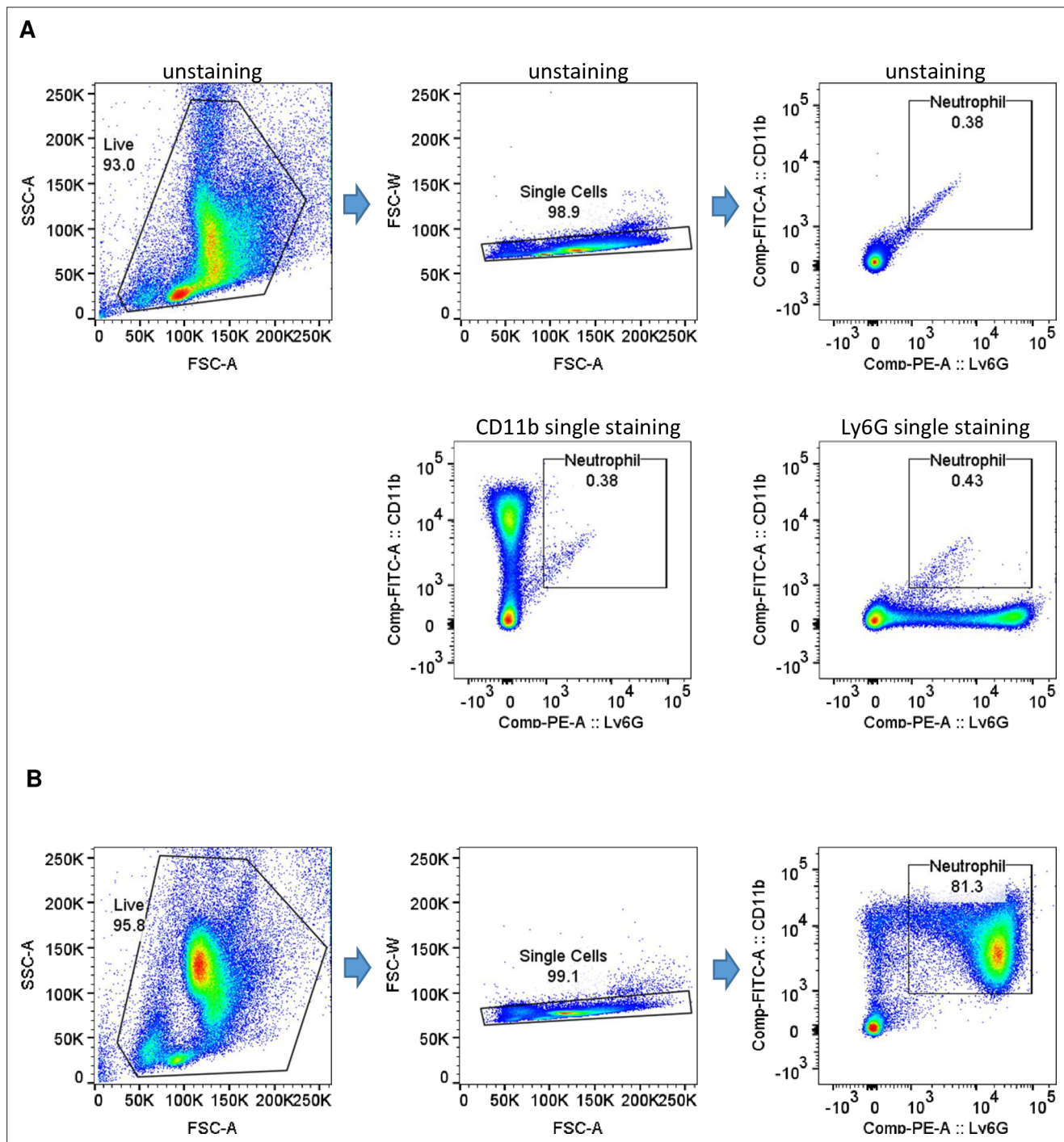
Figure 5—figure supplement 1. Gating strategy and purity of isolated neutrophil fractions. (**A**) Gating strategy. (**B**) Purity of isolated neutrophil fractions.
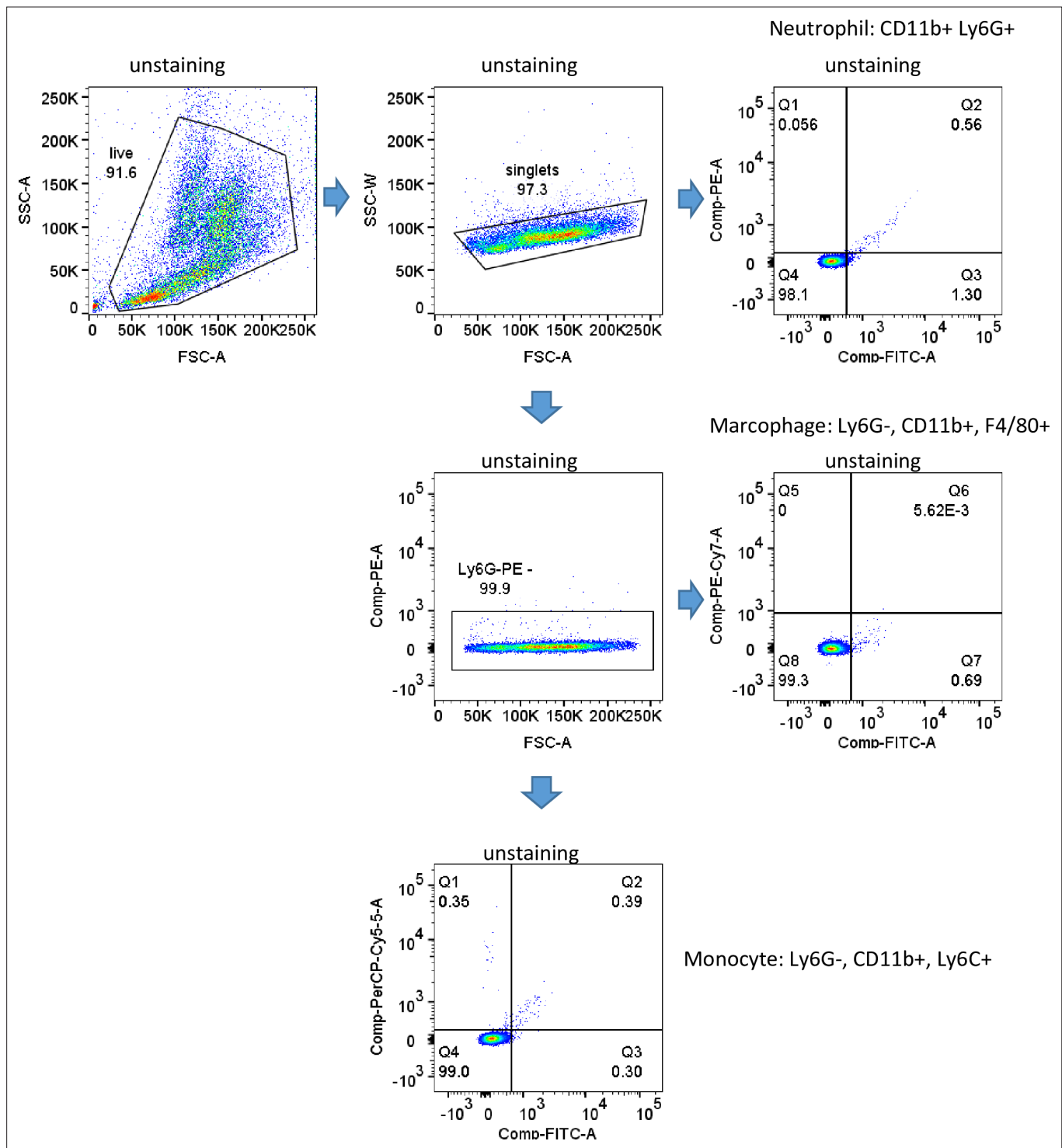
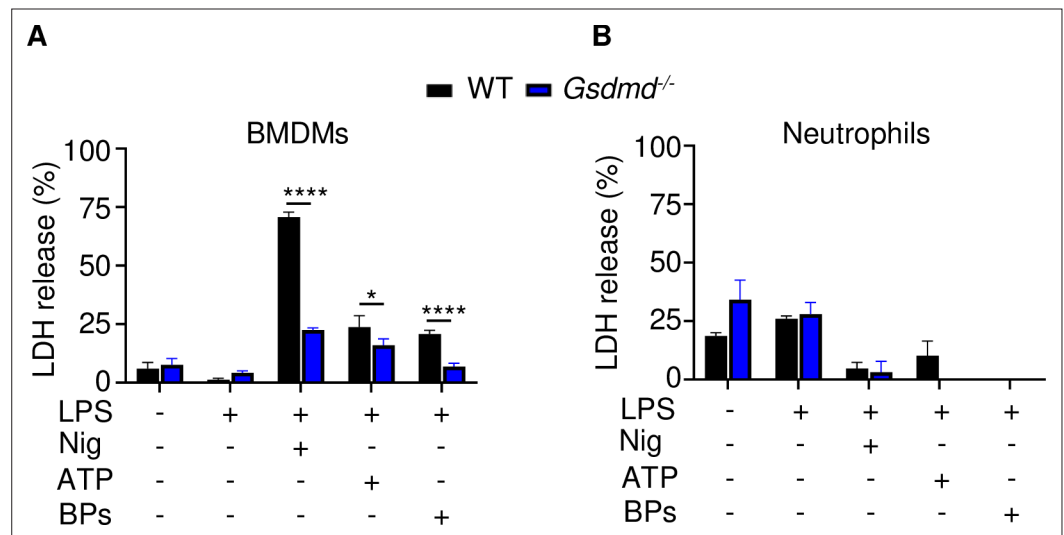**Figure 5—figure supplement 2.** Gating strategy.

Figure 5—figure supplement 3. Effects of GSDMD loss on LDH release. Bone marrow cells were isolated from 12-week-old male WT or *Gsdmd*^{-/-} mice. Bone marrow-derived macrophages (BMDMs) (**A**) were expanded in vitro whereas neutrophils (**B**) were used immediately after purification. Cells were primed with 100 ng/ml LPS for 3 hr, then with 15 μM nigericin for 1 hr, 5 mM ATP for 1 hr, or 50 mg/ml bone particles for 2 hr. LDH was measured in conditioned medium. Data are mean ± SD of triplicates and were representative of at least three independent experiments. *p < 0.05; ****p < 0.0001, two-way ANOVA with Tukey's multiple comparisons test. BPs, bone particles; LDH, lactate dehydrogenase; WT, wild-type.
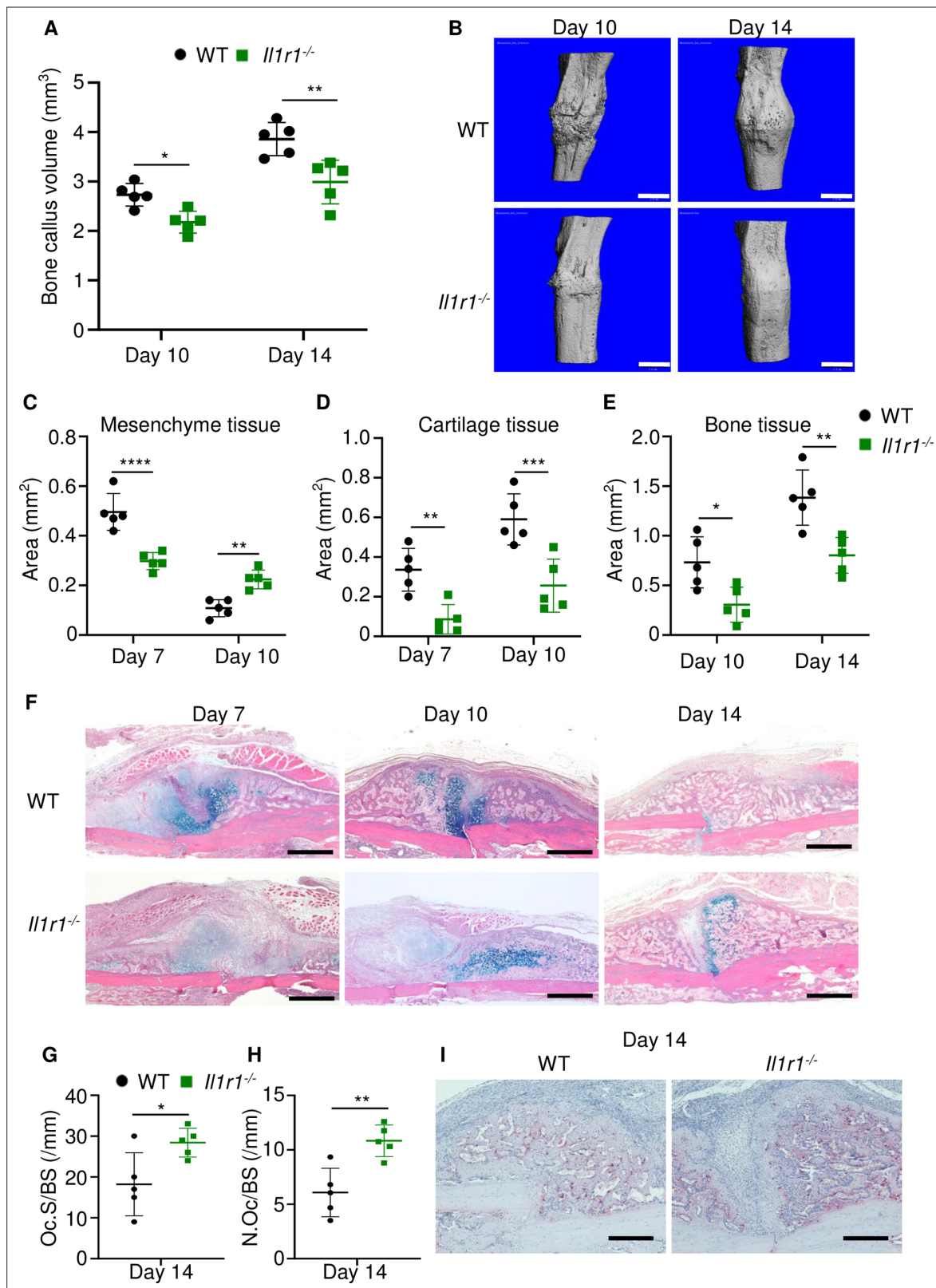
Figure 6. Loss of interleukin-1 (IL-1) receptor delayed fracture healing. Tibias of 12-week-old male WT or *Il1r1*$^{-/-}$ mice were subjected to fracture and analyzed at the indicated times. (**A**) Bone callus volume was quantified using Scanco software (n = 5). (**B**) Representative 3D reconstructions of bones using micro-computed tomography (μCT). (**C–E**) Quantification of tissue area by ImageJ software (n = 5). (**F**) Representative ABH staining. (**G**) Quantification of Oc.S/BS and (**H**) Oc.S/BS using Bioquant software (n = 5). (**I**) Representative images of TRAP staining. Data were mean ± SD.

Figure 6 continued on next page

Figure 6 continued

*p < 0.05; ***p < 0.001; ****p < 0.0001, two-way ANOVA with (**A, C–E**) Tukey's multiple comparisons test or (**G–H**) unpaired t-test. Scale bar, 1 mm (B), 500 μm, (F) or 200 μm (I). *Il1r1*, IL-1 receptor 1; WT, wild-type.
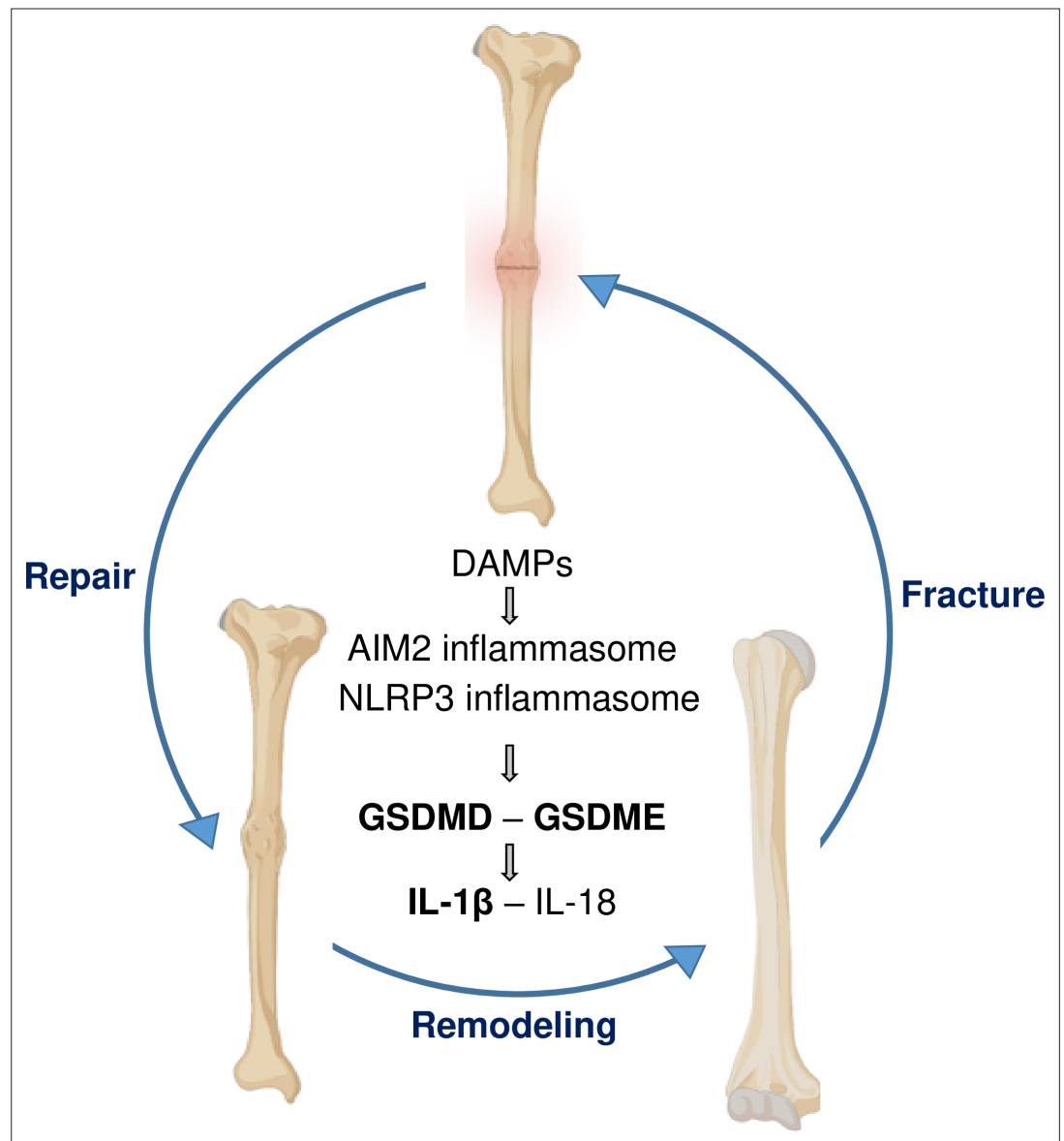
Figure 7. A model of gasdermin (GSDM)-interleukin-1 (IL-1) signaling in fracture healing. Bone fracture is followed by the repair and remodeling phases, which ultimately lead to the restoration of the original bone structure. Fracture causes the release of DAMPs, which activate the inflammasomes and other pathways, leading to the maturation of GSDMD and GSDME, and processing and secretion of IL-1β-IL-18. This model is based on the findings in bold texts indicating that mice lacking GSDMD, GSDME, or defective in IL-1 signaling (owing to the deletion of IL-1 receptor) exhibit delayed fracture healing. Levels of ATP (DAMP), AIM2, NLRP3, and IL-18 are elevated following fracture, but whether these factors are involved in fracture healing was not assessed in this study.